

# APPLICATIONS OF THE LOCAL OBSERVABLE IN FUTURE OPTICS MEASUREMENTS IN HL-LHC AND PETRA III

A. Wegscheider, R. Tomás, CERN, Geneva, Switzerland

## Abstract

Phase advances among four nearby beam position monitors in a circular accelerator can be used to calculate a local observable of quadrupolar lattice imperfections. This work explores the applicability of this local observable to two different circular accelerators: PETRA III, a synchrotron light source and the High Luminosity upgrade project of the CERNs Large Hadron Collider (HL-LHC). MAD-X simulations for relevant optics settings are performed, showing that the local observable can detect strong error sources. This is of particular interest in important regions of the accelerators like the LHC's interaction regions and PETRA III's experimental hall.

## INTRODUCTION

The measurement and control of the optics of an accelerator is a critical task for machine performance. Improving this aspect of accelerator operation is an ongoing task, as at the same time optics settings are constantly pushed further. With the introduction of more demanding lattice designs like in the case of the HL-LHC project, novel optics measurements and corrections methods are needed.

Special accelerator segments like the interaction regions of colliders need a precise control of local optics which becomes a challenging task for pushed beam optics designs as in, e.g. the HL-LHC.

In order to locate error sources we are interested in local observables, i.e., terms that only depend on lattice parameters and error sources in a localized region.

For linear lattice imperfections such an observable has been found recently [1], yielding promising characteristics for finding strong local error sources in the LHC.

The phase advance beating  $\Delta\varphi_{ab}$  between two elements of an accelerator  $a$  and  $b$  depends, in general, on all focusing errors around the ring

$$\begin{aligned} \Delta\varphi_{x,ab} = & \bar{h}_{ab} - 8 \sin^2 \varphi_{x,ab}^m \mathcal{R} \{f_a\} \\ & - 8 \sin \varphi_{x,ab}^m \cos \varphi_{x,ab}^m \mathcal{I} \{f_a\} \\ & + O(f^2). \end{aligned} \quad (1)$$

In the equation above,  $f_a$  denotes focusing resonance driving terms

$$f_a = \frac{\sum_w^W \delta K_{1,w} \beta_{x,w}^m e^{2i\varphi_{w,a}}}{8(1 - e^{4\pi i Q_x})}, \quad (2)$$

where  $\delta K_{1,w}$  is the deviation in integrated quadrupolar field strength for element  $w$  w.r.t. the model,  $\beta_{x,w}$  is the horizontal  $\beta$  function, and

$$\bar{h}_{ab} = \sum_{w \in I(a,b)} \beta_{x,w}^m \delta K_{1,w} \sin^2 \varphi_{x,w}^m. \quad (3)$$

$I(a, b)$  denotes the interval  $[\min(a, b), \max(a, b)]$ , superscript  $m$  denotes model values and  $O(f^2)$  collects all higher order terms of  $f_a$ , such as  $|f_a|^2$ ,  $\mathcal{R} \{f_a\}^2$ ,  $\mathcal{R} \{f_a\} \mathcal{I} \{f_a\}$  etc. Note that in this work we focus on calculations of the horizontal plane and therefore we omit the subscript  $x$  in the following. Calculations for the vertical plane are analogous.

The Resonance Driving Terms (RDTs)  $f_a$  are global, i.e. they include contributions from all elements with gradient errors  $\delta K_1$  in the machine. A careful resummation of different phase beatings yields a purely local term

$$\begin{aligned} \phi_{ijkl}^{meas} = & \cot \varphi_{jl}^m \Delta\varphi_{jl} - \cot \varphi_{jk}^m \Delta\varphi_{jk} \\ & + \cot \varphi_{ik}^m \Delta\varphi_{ik} - \cot \varphi_{il}^m \Delta\varphi_{il}. \end{aligned} \quad (4)$$

This term is equivalent to the analytic expression

$$\begin{aligned} \Phi_{ijkl}^{model} = & \cot \varphi_{jl}^m (\bar{h}_{il} - \bar{h}_{ij}) - \cot \varphi_{jk}^m (\bar{h}_{ij} - \bar{h}_{ik}) \\ & + \cot \varphi_{ik}^m \bar{h}_{ik} + \cot \varphi_{il}^m \bar{h}_{il} + O(f^2). \end{aligned} \quad (5)$$

In the case of model phase advances  $\varphi_{ij}^m$  of exact multiples of  $\pi$  the local observable simplifies to

$$\Delta\varphi_{ij} = \bar{h}_{ij}. \quad (6)$$

Since this case has the smallest error propagation, it is preferred but those exact phase advances will, in general, not appear frequently in the lattice.

The local observable is foreseen to be used to localise strong errors in Run 3 of LHC's operation and for its High Luminosity Upgrade. In this article, the merit of the linear local observable is demonstrated for several HL-LHC optics settings, is investigated.

## HL-LHC

A set of simulations is performed to assess the quality of the local observable in the HL-LHC. In order to reproduce a realistic measurement environment, noise levels that are present in current LHC measurements are introduced as well as magnet errors based on first measurements [2–4], cf Table 1. All but the strong error in MQ.22R4 are Gaussian distributed with the given standard deviation  $\sigma_{K_1}$ .

All plots in the following paragraphs show the local observable for the horizontal plane. The vertical local observable behaves similarly, only in the case of flat optics the asymmetry of the two planes has to be taken into account.

For the  $\pi$  phase advance case, a threshold  $\delta = 10^{-4} \times 2\pi$  rad is imposed, i.e.  $\Delta\varphi_{ij}$  is taken for the closest pair  $i, j$  for which  $\varphi_{ij}^m \in [\pi - \delta, \pi + \delta]$  holds.

## Injection Optics

Figure 1 shows the comparison between analytic formula and measured values from simulations for a typical noise

Table 1: HL-LHC Design Error Distribution

Element	$\delta K_1/K_1 [10^{-4}]$	$\sigma_{K_1}/K [10^{-4}]$
MQ	-	12
MQ.22R4	100	-
MQT	-	75
MQM	-	12
MQY	-	11
MQW	-	15
MQX	-	2
MB	-	12

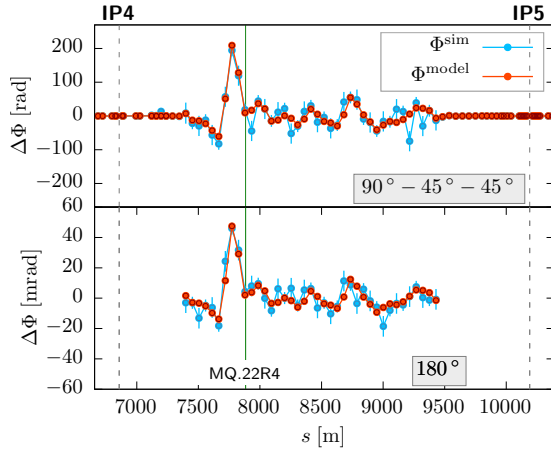


Figure 1: The local observable for a single strong error in Arc45. The error in MQ.22R4 is 1% of its nominal strength. The top plot shows simulated  $\Phi_{ijkl}^{meas}$  from Eq. (4) (blue graph) and  $\Phi_{ijkl}^{model}$  from Eq. (5) (red graph). The bottom plot show the case of an exact  $\pi$  model phase advance, Eq. (6). The regions around the IPs are free from  $\pi$  local observables since no candidates were found.

distribution in the HL-LHC at injection optics. The strong error introduced at quadrupole MQ.22R4 is clearly visible in the local observable. The top plot shows the local observable for combinations  $i, j, k, l$  where one BPM is skipped between  $i$  and  $j$ . The phase advance between consecutive BPMs in the (HL-)LHC is nearly  $45^\circ$  so this results in (approximate) model phase advances  $\varphi_{ij} = 90^\circ$ ,  $\varphi_{jk} = 45^\circ$  and  $\varphi_{kl} = 45^\circ$ . The bottom plot shows the case of exact multiples of  $\pi$ , as given by Eq. (6).

### Collision Optics

A far more challenging case is a collision optics with telescopic squeezing and large  $\beta$  functions in the final focus quadrupoles.

Figure 2 shows the simulated measurement for round collision optics with  $\beta^* = 15$  cm. The noise floor is considerably larger and the strong error source is not as clearly visible as for the injection optics. Also final focus errors play a stronger role because they leak second order effects (which

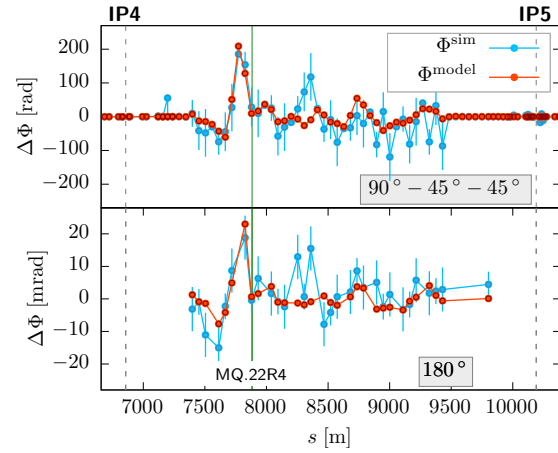


Figure 2: The same comparison as in Fig. 1 but with round collision optics ( $\beta^* = 15$  cm). The noise floor starts to dominate and a clear distinction of the strong error becomes difficult.

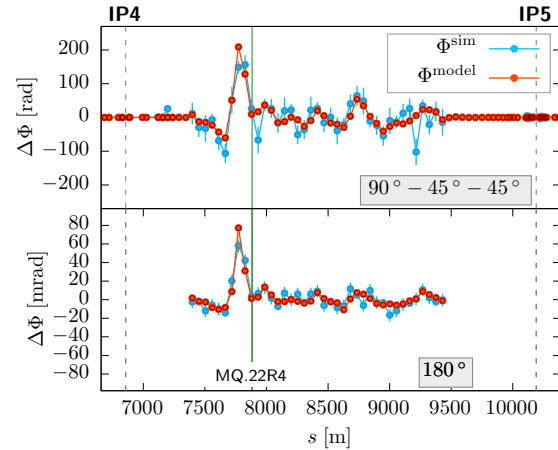


Figure 3: The same comparison as in Fig. 1 but with flat collision optics ( $\beta_x^* = 30$  cm,  $\beta_y^* = 7.5$  cm in IP5). The agreement for the  $180^\circ$  case is excellent.

include global contributions that cannot be eliminated) into the local observable.

Local observable measurements for the flat optics look more promising as can be seen in Fig. 3, at least for the plane with the larger  $\beta^*$ . The measurement precision of the  $\pi$  model phase advance case is better than for injection optics due to model phase advances closer to  $\pi$  in the telescopic arcs.

As for the LHC case [1], phase measurement noise prevents us from detecting design errors.

The noise can be reduced with better BPM resolution or a longer AC-dipole excitation. DOROS BPMs [5], currently introduced in the interaction regions, could significantly increase the phase resolution.

## PETRA III

A second study has been performed on the PETRA III lattice. The phase measurement at PETRA III turned out to be difficult because of the need to apply moving average filters to the LIBRA BPMs in order to obtain a sufficiently clean signal for turn-by-turn measurements.

Past measurements [6] and ongoing measurement activities at DESY showed a phase advance measurement precision not better than 1.0 mrad. The following simulation shows a phase noise corresponding to an optimistic prediction that such a precision can be achieved in any future measurement.

The FODO cells of PETRA III have a phase advance of  $72^\circ$  and thus the clean  $90^\circ - 45^\circ - 45^\circ$  setup that was used for the LHC cases is not possible here. Therefore most local observables lie closer to  $72^\circ - 150^\circ - 72^\circ$  whereas the distribution of combinations in the experimental hall is more diverse.

As error distribution we assumed 10 units of  $10^{-4}$  in all quadrupoles around the ring as shown in Table 2. With this error distribution and the assumed phase measurement noise, measurement of the local observable is difficult, as can be seen in Fig. 4. The top plot shows the experimental hall and the bottom plot shows the first 1000 m of the accelerator, spanning several arcs.

Table 2: PETRA III Error Distribution

Element	$\delta K_1/K_1 [10^{-4}]$	$\sigma_{K_1}/K [10^{-4}]$
Q	-	10
QA2_NOR_71	100	-

Single strong errors of  $\approx 1\%$ , on the other hand, are well measurable above the noise background, as can be seen in Fig. 5. The strong error is clearly visible above the noise background. An outlier is visible, most likely due to unsuitable phase advances in this particular combination.

## CONCLUSION

The HL-LHC optics is more challenging for our measurement and correction tools than any of today's configuration of the LHC. Novel measurement methods are in order to maintain the needed accuracy and precision and to meet the requirements imposed on optics corrections. The local observable is one candidate of such measurement methods, enabling us to locate strong error sources in the arcs. With the current accuracy and precision of phase measurements, the detection of strong error sources should be performed with injection optics, as the picture is not as clear in collision. Ideally we would want to perform the measurements for all optics settings as some errors only get apparent in certain optics. A foreseen BPM upgrade, longer AC-dipole excitation and increased statistics (e.g. through the excitation of three bunches instead of one) could yield more precise local observable measurements and, thus, allow the consideration of any optics setting.

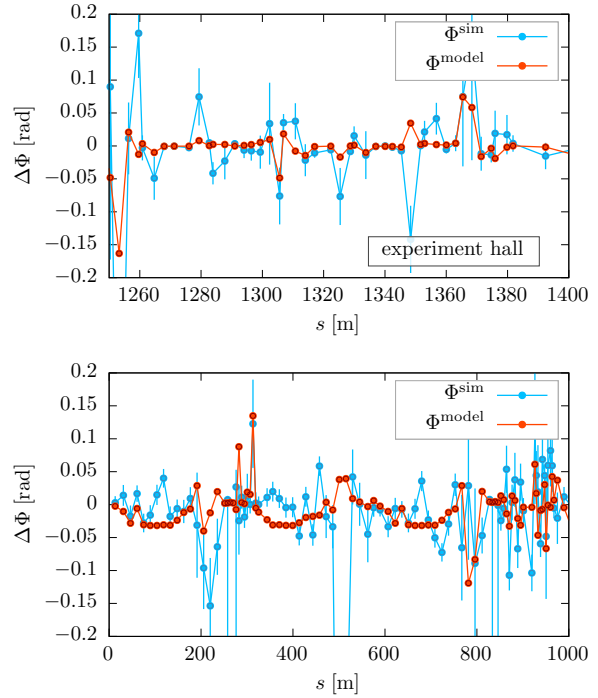


Figure 4: The local observable in PETRA III. The top plot shows the experimental hall, the bottom plot shows the first 1000 m of the accelerator. With the assumed phase measurement precision, the given error distribution is not measurable.

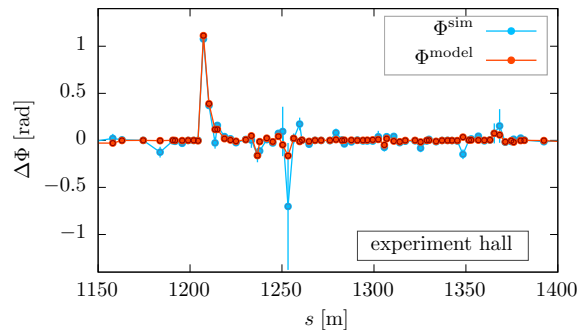


Figure 5: Strong errors of  $\approx 1\%$  relative error are clearly visible above the noise background.

The detection of strong error sources in PETRA III is perfectly feasible according to our studies. A better control of the phase measurement could bring an additional gain in precision and sub-percent error sources could be achievable in the future.

## ACKNOWLEDGMENTS

Research supported by the HL-LHC project. We want to warmly thank I. Agapov and the team from DESY for their help.

## REFERENCES

- [1] A. Wegscheider and R. Tomás, “Local observable for linear lattice imperfections in circular accelerators”, *Phys. Rev. Accel. Beams*, vol. 23, p. 054002, 2020. doi:10.1103/PhysRevAccelBeams.23.054002
- [2] E. Todesco *et al.*, “Update on IR magnets field quality: nested correctors and spread of TF in quadrupoles”, presented at the 186th HiLumi WP2 Meeting, Virtual Meeting, CERN, Geneva, Switzerland, Dec. 2020, unpublished.
- [3] E. Todesco *et al.*, “Interface specification WP2/WP3, Accuracy and precision of magnetic measurements”, CERN, Geneva, Switzerland, Rep. LHC-M-ES-0016, 2020.
- [4] L. Fiscarelli *et al.*, “Field Quality of MBH 11-T Dipoles for HL-LHC and Impact on Beam Dynamic Aperture”, *IEEE Trans. Appl. Supercond.*, vol. 28, p. 4004005, 2018. doi:10.1109/TASC.2018.2792424
- [5] M. Gasior, J. Olexa, and R. J. Steinhagen, “A High-resolution Diode-based Orbit Measurement System – Prototype Results from the LHC”, in *Proc. 10th European Workshop on Beam Diagnostics and Instrumentation for Particle Accelerators (DI-PAC'11)*, Hamburg, Germany, May 2011, paper MOPD24, pp. 98–100.
- [6] I. V. Agapov *et al.*, “Linear and Nonlinear Optics Measurements With Multiturn Data at PETRA III”, in *Proc. 8th Int. Particle Accelerator Conf. (IPAC'17)*, Copenhagen, Denmark, May 2017, pp. 170–173. doi:10.18429/JACoW-IPAC2017-MOPAB040